JOURNAL OF SOLID STATE CHEMISTRY 120, 23–31 (1995)

The Crystal Structure of α- and β-$Na_2CuP_2O_7$

Fatima Erragh,* Ali Boukhari,* Francis Abraham,† and Brahim Elouadi*,[1]

*Applied Solid State Chemistry Laboratory, Faculty of Science, Charia Ibn Batota, Rabat, Morocco; and †Laboratoire de Cristallochimie et Physicochimie du Solide, Université de Lille I, Ecole Nationale Supérieure de Chimie de Lille, B.P.108, 59652 Villeneuve d'Ascq, France

Received October 4, 1994; accepted June 8, 1995

The crystal structures of both α- and β-modifications of copper disodium diphosphate ($Na_2CuP_2O_7$) were solved at 295 K. The low-temperature phase α-$Na_2CuP_2O_7$ has been found to undergo an irreversible phase transition to β-$Na_2CuP_2O_7$, at 843 K. The α-allomorph crystallizes with a faint blue color and the space group $P2_1/n$ ($Z = 4$) with unit cell parameters $a = 8.823(3)$, $b = 13.494(3)$, $c = 5.108(2)$ Å, and $\beta = 92.77(3)°$. Single crystals of the high-temperature form β-$Na_2CuP_2O_7$, recognized by their dark blue color, have also a monoclinic symmetry with the space group $C2/c$ ($Z = 4$) and unit cell parameters $a = 14.728(3)$, $b = 5.698(1)$, $c = 8.067(1)$ Å, and $\beta = 115.15(1)°$. The structure parameters were refined to a final R of 0.020 ($wR = 0.031$) for 1550 independent reflections [$I > 3\sigma(I)$] in the case of α-$Na_2CuP_2O_7$ (α-NCP) and a final R of 0.024 ($wR = 0.043$) for 1234 independent reflections [$I > 3\sigma(I)$] in the case of β-$Na_2CuP_2O_7$ (β-NCP). Both α- and β-NCP structures are built up of infinite ribbons $[CuP_2O_7]_n^{2n-}$ made of alternating diphosphate groups $(P_2O_7)^{4-}$ and Cu^{2+} cations. Each copper cation is connected to two adjacent $(P_2O_7)^{4-}$ groups via two oxygens belonging to two different [PO_4] tetrahedra. The main structural differences between the two networks reside in the shape of the ribbons (corrugated or flat) and the way the sodium cations are set out between appropriate ribbons. In β-$Na_2CuP_2O_7$ all the ribbons are corrugated and stacked in layers connected to each other by sheets of Na^+ parallel to (100). The lattice may then be regarded as having a lamellar character. The low-temperature form can be seen as made of infinite pairs of $[CuP_2O_7]_n^{2n-}$ flat ribbons embedded in a matrix of Na^+. In the latter phase, the ribbons, running parallel to [001], are symmetrically related by a center of inversion and a glide plane n belonging to the space group $P2_1/n$. The mean values of the bond lengths in β-NCP are all smaller than equivalent ones in the low-temperature modification. Furthermore all diphosphate groups adopt an almost eclipsed configuration in both allomorphs. The P–O–P angle, equal to 118.66° in α-$Na_2CuP_2O_7$, represents the smallest value found for all diphosphates so far known. The copper coordination is square-pyramid-like in the α-NCP phase, while it is of planar square type in the β-NCP variety.

[1] To whom correspondence should be addressed at Université de La Rochelle, Département de Chimie, Avenue Marillac, 17042 La Rochelle Cédex 01, France.

I. INTRODUCTION

The title compound is part of a broad research program conducted in our laboratory for almost a decade on both crystalline and vitreous pyrophosphates isolated within the binary diagrams $A_4^IP_2O_7$–$B_2^{II}P_2O_7$, where A^I and B^{II} stand for monovalent and divalent cations, respectively (1–10). The diphosphates $A_2^IB^{II}P_2O_7$ were subject to various studies but few of them have concerned structural determination on single crystals (4–6, 11–22). Prior to our investigations, the structure of $Na_7Mg_{4.5}(P_2O_7)_4$, determined on a single crystal, was the only one reported for the sodium systems (11–12). Refinements of the structure carried out on newly grown crystals of $Na_{7.13}Mg_{4.36}(P_2O_7)_4$ and $Na_{7.39}Ni_{4.24}(P_2O_7)_4$ have allowed us to confirm a close resemblance between their structural types, although their chemical formulas are slightly different (3, 6). We have also grown single crystals within various systems (A = Na; B = Co, Zn, etc.) and have solved the structures of some of them, while other studies are in progress (3–6).

The purpose of the present paper is to report the resolved crystal structures of two varieties of $Na_2CuP_2O_7$ in order to contribute to a better insight into the crystal chemistry of mixed mono- and divalent pyrophosphates. Furthermore, among all the divalent cations examined, Cu^{2+} is expected to play a special role, due to the Jahn–Teller effect related to its d^9 configuration. Since the latter cations can normally accommodate intermediate coordinations between the octahedral one and that of a planar square, it is of importance to investigate the structural types adopted by the phases prepared and particularly to make clear the effect of the Jahn–Teller deformation on the mutual orientations of the two PO_4 tetrahedra within the pyrophosphate groups $(P_2O_7)^{4-}$.

II. CRYSTAL GROWTH AND DATA COLLECTION

Two different methods were successfully used for the growth of single crystals of both α- and β-$Na_2CuP_2O_7$:

(a) $Cu_2P_2O_7$ and $Na_4P_2O_7$, initially synthesized from pro-analysis grade starting materials CuO, Na_2CO_3, and

0022-4596/95 $12.00

$(NH_4)_2HPO_4$, were mixed (molar ratio of 2/3) and intimately ground in an agate mortar before melted at 943 K. The resulting bath was then slowly cooled (5 Kh^{-1}) down to 673 K before the furnace was switched off to allow the temperature of the whole system to continuously decrease to 293 K. The collected crystals were of two types: those of α-$Na_2CuP_2O_7$ (α-NCP) were faint blue and those corresponding to β-$Na_2CuP_2O_7$ (β-NCP) had a dark blue color.

(b) The melt of a mixture of Na_2CO_3, CuO, and $(NH_4)_2HPO_4$ corresponding to the stoichiometric compound $Na_2CuP_2O_7$ was cooled, with a rate of 5 K per hr, from 943 to 473 K. The furnace was then turned off in order to allow the temperature to reach 293 K, according to the thermal inertia of the oven. The crystals obtained were identical to those previously labeled β-$Na_2CuP_2O_7$.

The crystals of both α- and β-$Na_2CuP_2O_7$ used for the structural studies have parallelepipedic shapes with approximate dimensions of $26 \times 125 \times 320$ and $104 \times 86 \times 350\ \mu m^3$, respectively. Weissenberg photographs have shown that the reflection conditions are compatible with the space groups $P2_1/n$ for α-$Na_2CuP_2O_7$ and $C2/c$ or Cc for β-$Na_2CuP_2O_7$. The exact values of the unit cell parameters were obtained by least-squares refinement from powder X-ray diffraction patterns collected with a C. G. R.-Θ60 diffractometer.

Intensities were collected on a Philips PW 1100 four-circle diffractometer using Mo$K\alpha$ radiation ($\lambda_{K\alpha}$ = 0,7107 Å), selected with a graphite monochromator. All data were corrected for Lorentz and polarization effects. Absorption corrections were performed using the analytical method of Meulenaer and Tompa (23), while atomic scattering factors were taken from the "International Tables for X-ray Crystallography" (24). Anomalous dispersion corrections were made according to the method suggested by Cromer and Liberman (25). The full-matrix least-square refinements were performed using an adapted version of the SFLS-5 program (26). The conditions of the data collections and structure refinements for both α- and β-$Na_2CuP_2O_7$ are recapitulated in Table 1. Atomic coordinates and selected interatomic distances and bond angles are given in Tables 2, 3, and 4.

III. DESCRIPTION OF THE STRUCTURES

The projection of α-$Na_2CuP_2O_7$ on (001) is given in Fig. 1a. As shown from Fig. 1b, the structure can be viewed as made of infinite arrangements of two diphosphate groups ($P_2O_7^{4-}$) connected through a copper atom and the resulting chemical formula is $(CuP_2O_7)_n^{2n-}$. Such arrangements give rise to identical infinite ribbons (labelled A_α or B_α, depending on their orientation within the lattice), expanding along [001], and symmetrically related as follows: (a) ribbons A_α and B_α are connected through the glide plane n; (b) ribbons of the same orientation (A_α or B_α) are related by a center of symmetry. The overall structure can be seen as made of ribbon pairs of type A_α and B_α embedded in a matrix of sodium cations. Therefore, the structural role of Na^+ cations function only to maintain charge neutrality and to sustain the ribbons from bending or collapse. The structure can also be regarded as corrugated sheets, stacked along [010], and attached by sodium ions (Fig. 1c). The sheets are made of flat $(CuP_2O_7)_n^{2n-}$ ribbons running along [100] as shown in Fig. 1d.

The structure of β-$Na_2CuP_2O_7$, seen along [100] direction, is represented in Fig. 2a. The structure can be seen as formed of corrugated ribbons $(CuP_2O_7)_n^{2n-}$. As in α-$Na_2CuP_2O_7$, the latter are built of infinite arrangements of Cu(II) and $(P_2O_7)^{2-}$ where each copper is connected to two adjacent diphosphate groups. However, the resulting ribbons labelled C_β have a totally different configuration due to the rippling of $(CuP_2O_7)_n^{2n-}$ strips. Furthermore, the whole structure contains the same type of ribbons shaped like layers parallel to (100) and related through lattice translation only. The lamellar character of the structure appears evident when it is noticed that the sheets of ribbons are connected by layers of sodium cations.

IV. DISCUSSION OF THE CHEMICAL BOND

The diphosphate anions are built up of identical $[PO_4]$ phosphate tetrahedra in β-$Na_2CuP_2O_7$. In contrast, those of α-NCP contain two types of $[PO_4]$ slightly different in size (Table 3). Although the average P–O distances are practically identical in both polymorphs (1.544 Å for α- and 1.542 Å for β-NCP), the $[PO_4]$ polyhedra are far from being regular. The distortions observed have been tentatively explained on the basis of the chemical bonds and the electrostatic repulsions between electronic doublets (or electronic clouds) according to Gillespie's model (27). It is also noteworthy that the longest bonds in the tetrahedra $[PO_4]$ are always found along P–O–P bridges. Among the six terminal P–O bonds of a diphosphate group, the shortest concern oxygens which either are not or are weakly connected to copper atoms as is the case for O(2) in β-NCP and O(5) or O(6) in the α- modification.

As may be expected from energetic considerations and atomic orbital combinations, the bond length is inversely proportional to the bond strength. Therefore, the shortest distance P–O in both polymorphs corresponds to P=O with a double bond character, resulting from $d\pi$-$p\pi$ overlap (28, 29). Furthermore, two oxygens of each $[PO_4]$ are used to link the phosphorus to the two neighboring copper cations, while the last one is shared between two adjacent phosphorus in order to build up the diphosphate bridge. In all the latter cases, the P–O bonds involved are only of σ type. The mean value of $P–O_{br}$ (br = bridge) close to 1.543 Å reveals a linear P–O–P (as in thortveitite structural type) while a greater value is compatible with angular

TABLE 1
Crystal Data, Intensity Measurements, and Structure Refinement Parameters

Compound	α-$Na_2CuP_2O_7$	β-$Na_2CuP_2O_7$
Crystal data		
Crystal system	Monoclinic	Monoclinic
Space group	$P2_1/n$	$C2/c$
Cell dimensions		
a(Å)	8.823(3)	14.728(3)
b(Å)	13.494(3)	5.698(1)
c(Å)	5.108(2)	8.067(1)
β(°)	92.77(3)	115.15(1)
Cell volume (Å^3)	607.5	612.8
Z	4	4
Dcalc. (g·cm^{-3})	3.10	3.07
Dexp(g·cm^{-3})	3.15(5)	3.07(5)
Crystal color	Light blue	Dark blue
Data collection		
Equipment	Philips PW 1100	Philips PW 1100
λ[Mo$K\alpha$ (graphite monochromator)]	0.7107 Å	0.7107 Å
Temperature (K)	295	295
Scan mode	$\omega - 2\Theta$	$\omega - 2\Theta$
Scan width (°)	1.2	1.2
Θ range (°)	2–30	2–35
Standard reflections measured every 2 hr (no decay)	$\bar{1}\bar{2}1$; $\bar{1}\bar{3}0$; $\bar{1}\bar{1}\bar{1}$	310; $\bar{4}02$; $\bar{3}10$
Recording reciprocal space	$-12 \le h \le +12$; $-18 \le k \le +18$; $0 \le l \le 7$	$-23 \le h \le +23$; $-9 \le k \le +9$; $0 \le l \le 13$
No. of reflections measured	3756	2462
No. of reflections [$I > 3\sigma(I)$]	3253	2286
No. of independent reflections	1550	1234
μ(cm^{-1}) for λMo$K\alpha$ = 0.7107 Å	43.9	43.4
Limiting faces (hkl) and distances (mm) from an arbitrary origin	(110), $(1\bar{1}0)$ 0.013 $(1\bar{1}0)$, $(\bar{1}10)$ 0.062 (001), $(00\bar{1})$ 0.160	(100), $(\bar{1}00)$ 0.043 (010), $(0\bar{1}0)$ 0.052 $(01\bar{1})$, $(0\bar{1}1)$ 0.175
Transmission factor range	0.56–0.89	0.32–0.69
Merging R factor	0.016	0.016
Refinement		
No. of parameters refined	109	57
$R = \sum [\lvert F_o \rvert - \lvert F_c \rvert] / \sum \lvert F_o \rvert$	0.020	0.024
$Rw = [\sum w(\lvert F_o \rvert - \lvert F_c \rvert)^2 / \sum F_o^2]^{1/2}$ with $w = 1/\sigma(F_o)$	0.031	0.043

P–O–P bridges (30). The P–O_{br} lengths found for P(1)–O(7), P(2)–O(7) and P–O(4) (respectively equal to 1.633, 1.613, and 1.616 Å), are totally compatible with the small values of the diphosphate bridge angles: P(1)–O(7)–P(2) (Fig. 1b) in α-NCP and P–O(4)–P (Fig. 2a) in β-NCP are equal to 118.7° and 120.1°, respectively. These values are then consistent with a high bending of the P–O–P bridges in both polymorphs (30). Moreover, these angles are among the lowest reported for all diphosphate groups investigated so far (3, 5, 12, 17, 30–36). Amidst the pyrophosphates having small P–O–P bond angles close to the values found for the title compound, we can quote: $Li_2PdP_2O_7$ (120.0°), $Na_2PdP_2O_7$ (122.0°), $KAlP_2O_7$ (123.2°), $KFeP_2O_7$ (124.3°), $BaCuP_2O_7$ (122.1°), etc. (16, 17, 31, 32). The angle P(1)–O(7)–P(2) found in α-NCP (Fig. 1b) appears to be the smallest bridge angle (118.7°) ever reported for any diphosphate group so far brought to our knowledge.

The angles O–P–O involving a double bond P=O (for instance, O(3)–P(1)–O(5) or O(1)–P(2)–O(6) in α-NCP and O(1)–P–O(2) in the β-phase, etc.) are found systemati-

TABLE 2
Atomic Coordinates and Equivalent Isotropic Temperature Factors for the Two Modifications of $Na_2CuP_2O_7$

Compound and color	Atoms	x	y	z	$\beta_{eq}(Å)^2$
α-$Na_2CuP_2O_7$ (light blue)	Cu	0.25768(3)	0.15840(2)	0.20512(5)	0.77
	P(1)	0.72850(6)	0.46307(4)	0.20705(10)	0.70
	P(2)	0.95594(6)	0.31901(4)	0.22880(10)	0.67
	Na(1)	0.6517(1)	0.2082(1)	0.2335(2)	1.22
	Na(2)	0.1308(1)	0.8902(1)	0.2188(2)	1.49
	O(1)	0.9119(2)	0.2756(1)	0.4915(3)	0.95
	O(2)	0.8603(2)	0.2741(1)	0.0019(3)	0.89
	O(3)	0.6785(2)	0.4470(1)	−0.0808(3)	1.04
	O(4)	0.6503(2)	0.3873(1)	0.3816(2)	0.89
	O(5)	0.7153(2)	0.5674(1)	0.2945(3)	1.35
	O(6)	0.1232(2)	0.3120(1)	0.1925(3)	1.14
	O(7)	0.9084(2)	0.4344(1)	0.2344(3)	0.93
β-$Na_2CuP_2O_7$ (dark blue)	Cu	0	0	0	0.87
	P	0.10478(3)	0.34114(7)	−0.15575(5)	0.63
	Na	0.27068(6)	0.6399(1)	0.2009(1)	1.18
	O(1)	0.1017(1)	0.2135(2)	0.0077(2)	1.26
	O(2)	0.1878(1)	0.5160(2)	−0.1017(2)	1.00
	O(3)	0.1072(1)	0.1677(2)	−0.2994(2)	1.29
	O(4)	0	0.4825(3)	−1/4	0.82

Note. $\beta_{eq} = \frac{4}{3} \sum_i \sum_j \beta_{ij} \alpha_i \alpha_j$.

cally larger than those containing only simple bonds like O(1)–P(2)–O(2) or O(3)–P(1)–O(4) in α-NCP and O(3)–P–O(1) in β-NCP (see Tables 3 and 4). These results are compatible with Gillespie's model which predicts that the enlargement of a bond angle results from the increment of the electrostatic repulsions between the electronic clouds of the chemical bonds involved (27). Since the latter forces are proportional to the number of electronic doublets engaged in the bonds, it is therefore obvious that the angles made between two simple bonds P–O will be smaller than the one formed by P–O and a double bond P=O within the same tetrahedron [PO_4]. Furthermore, a nearly eclipsed configuration compatible with the dichromate structural type is adopted by the latter groups in both α- and β-NCP varieties (30, 37).

As evidenced from Figs. 1 and 2 and Tables 3 and 4, half of the [PO_4] apices are engaged in P–O–Cu bridges. Therefore, the magnitudes of the bond lengths and angles of the pyrophosphate groups are directly related to the bond strength within the coordination polyhedra of the adjacent copper cations. In the α-allomorph, the latter atoms are located in highly deformed octahedra made of O(1), O(2), O(3), O(4), O(6), and O(7), while in β-NCP, copper(II) ions are inserted in planar square-like cavities O(1)–O(3)–O(1)–O(3) as shown in Fig. 2a. A close examination of the local structure in the vicinity of Cu^{2+} in both α- and β-NCP modifications, allows the following conclusions:

—Concerning α-$Na_2CuP_2O_7$, the oxygen atoms O(7), situated at a distance of 3.07 Å from copper(II), can be drawn out from the coordination octahedra since the interaction Cu–O(7) is not significant. However, due to irregular values of the angles O(6)–Cu–O(i) (i = 1, 2, 3, 4) varying from 80° (i = 2) to 117.3° (i = 3), the resulting coordination polyhedron [CuO_5] cannot be assimilated to a simple square pyramid even though the rapprochement is tempting.

—In β-$Na_2CuP_2O_7$, the deformed octahedron representing the coordination site of copper(II) is composed of the following oxygens (Fig. 2): O(1)x2, O(3)x2 and O(4)x2. Since the distance Cu^{2+}–O(4) is particularly long (3.410 Å), the coordination polyhedra of Cu^{2+} are therefore reduced to planar square-like cavities.

Due to Jahn–Teller distortions inherent to Cu^{2+}, the environment of the latter cations is not expected to be regular (38). This is compatible with the dissimilar values of the bond lengths and angles found for both α- and β-NCP (Tables 3 and 4). Moreover, since copper coordination polyhedra are sandwiched between two diphosphate groups, it appears that the elongation of Cu–O bonds is compensated by a shortening of the adjacent P–O distances. This is proven by the almost identical spans of the following chains: (a) In α-$Na_2CuP_2O_7$ (Fig. 1b);

$$P(1)–O(3)–Cu–O(1)–P(2) = 7.000 Å \quad [1]$$

TABLE 3
Main Interatomic Distances (Å) and Bond Angles (°) for α-$Na_2CuP_2O_7$

$Cu-O(1)^{ii}_{\bar{1}0\bar{1}} = 1.995(2)$	$Cu-O(4)^{ii}_{\bar{1}0\bar{1}} = 1.964(1)$
$Cu-O(2)^{ii}_{\bar{1}00} = 1.953(2)$	$Cu-O(6)^{i}_{\bar{1}00} = 2.388(1)$
$Cu-O(3)^{ii}_{\bar{1}00} = 1.944(2)$	$\langle Cu-O\rangle = 1.968$
$O(1)^{ii}_{\bar{1}0\bar{1}}-Cu-O(2)^{ii}_{\bar{1}00} = 85.02(11)$	$O(2)^{ii}_{\bar{1}00}-Cu-O(4)^{ii}_{\bar{1}0\bar{1}} = 170.46(11)$
$O(1)^{ii}_{\bar{1}0\bar{1}}-Cu-O(3)^{ii}_{\bar{1}00} = 155.14(42)$	$O(2)_{\bar{1}00}-Cu-O(6)^{i}_{\bar{1}00} = 80.10(9)$
$O(1)^{ii}_{\bar{1}0\bar{1}}-Cu-O(4)^{ii}_{\bar{1}0\bar{1}} = 89.67(11)$	$O(3)^{ii}_{\bar{1}00}-Cu-O(4)^{ii}_{\bar{1}0\bar{1}} = 94.12(10)$
$O(1)^{ii}_{\bar{1}0\bar{1}}-Cu-O(6)^{i}_{\bar{1}00} = 87.07(10)$	$O(3)_{\bar{1}00}-Cu-O(6)^{i}_{\bar{1}00} = 117.30(14)$
$O(2)^{ii}_{\bar{1}00}-Cu-O(3)^{ii}_{\bar{1}00} = 94.02(11)$	$O(4)^{ii}_{\bar{1}0\bar{1}}-Cu-O(6)^{i}_{\bar{1}00} = 91.73(9)$
$Na(1)-O(1)^{i} = 2.746(2)$	$Na(2)-O(1)^{iii}_{111} = 2.719(2)$
$Na(1)-O(1)^{ii}_{\bar{1}0\bar{1}} = 2.408(2)$	$Na(2)-O(2)^{iii}_{110} = 2.490(2)$
$Na(1)-O(2)^{i} = 2.406(2)$	$Na(2)-O(3)^{iii}_{1\bar{1}0} = 2.459(2)$
$Na(1)-O(2)^{ii}_{\bar{1}00} = 2.981(2)$	$Na(2)-O(4)^{iv} = 2.509(2)$
$Na(1)-O(4)^{i} = 2.532(2)$	$Na(2)-O(5)_{\bar{1}1\bar{1}} = 2.395(2)$
$Na(1)-O(5)^{iv}_{1\bar{1}0} = 2.241(2)$	$Na(2)-O(6)^{iv}_{\bar{1}00} = 2.436(2)$
$Na(1)-)(6)^{ii}_{\bar{1}0\bar{1}} = 2.776(2)$	$\langle Na(1)-O\rangle = 2.559$
$Na(1)-O(6)^{ii}_{\bar{1}00} = 2.386(2)$	$\langle Na(2)-O\rangle = 2.500$
$P(1)-O(3)^{i} = 1.530(2)$	$P(2)-O(1)^{i} = 1.531(2)$
$P(1)-O(4)^{i} = 1.541(1)$	$P(2)-O(2)^{i} = 1.526(2)$
$P(1)-O(5)^{i} = 1.483(2)$	$P(2)-O(6)^{i} = 1.499(2)$
$P(1)-O(7)^{i} = 1.633(2)$	$P(2)-O(7)^{i} = 1.613(1)$
$\langle P(1)-O\rangle = 1.547$	$\langle P(2)-O\rangle = 1.542$
$O(3)^{i}-P(1)-O(4)^{i} = 110.20(17)$	$O(1)^{i}-P(2)-O(2)^{i} = 111.07(19)$
$O(3)^{i}-P(1)-O(5)^{i} = 113.62(19)$	$O(1)^{i}-P(2)-O(6)^{i} = 112.11(21)$
$O(4)^{i}-P(1)-O(5)^{i} = 106.47(18)$	$O(1)^{i}-P(2)-O(7)^{i} = 106.06(16)$
$O(4)^{i}-P(1)-O(6)^{i} = 114.30(18)$	$O(2)^{i}-P(2)-O(6)^{i} = 113.16(22)$
$O(4)^{i}-P(1)-O(7)^{i} = 104.68(18)$	$O(2)^{i}-P(2)-O(7)^{i} = 105.16(22)$
$O(3)^{i}-P(1)-O(7)^{i} = 106.79(18)$	$O(6)^{i}-P(2)-O(7)^{i} = 108.75(19)$
$P(1)-O(7)-P(2) = 118.66(15)$	$\langle O-P-O\rangle = 109.36$

Note. Symmetry code (see Table 2 for the values of x, y, z): (i) $x\ y\ z$; (ii) $\frac{1}{2}+x, \frac{1}{2}-y, \frac{1}{2}+z$; (iii) $\bar{x}\ \bar{y}\ \bar{z}$; (iv) $\frac{1}{2}-x, \frac{1}{2}+y, \frac{1}{2}-z$.
$O(n)^{X}_{pqr}$ represents the oxygens $O(n)$ concerned with the above symmetry code X and the translation vector $p\mathbf{a} + q\mathbf{b} + r\mathbf{c}$.

$$P(2)-O(2)-Cu-O(4)-P(1) = 6.984\ \text{Å}. \quad [2]$$

(b) In β-$Na_2CuP_2O_7$ (Fig. 2a);

$$P-O(3)-Cu-O(1)-P = 6.940\ \text{Å}. \quad [3]$$

However, in the case of the latter modification (Fig. 2a), a noticeable difference is observed between the lengths of the bond chains equivalent to those given for α-NCP in Eqs. [1] and [2],

$$P-O(1)-Cu-O(1)-P = 6.876\ \text{Å} \quad [4]$$

$$P-O(3)-Cu-O(3)-P = 7.004\ \text{Å}. \quad [5]$$

The latter divergences displayed between the two structural types probably result from the nonequivalent *mechanical tensions taking place within the ribbons* $[CuP_2O_7]^{2n-}_n$ of both polymorphs. As a matter of fact, as shown in Fig. 3, the diphosphate groups are not oriented in the same way with regard to $[CuO_4]$ pseudo-squares. In *corrugated ribbons* (β-NCP), *the chains* P–O–Cu–O–P tend to align within the same plane, while in β-NCP furrows, having the shape and size of the angles O(1)–P(1)–O(2) and O(4)–P(2)–O(3), seem to be dug at the surface of the layers where all $[CuO_4]$ are aligned. Due to the above mentioned differences in configuration of the bonding within the chains P–O–Cu–O–P, it then appears clearly that the resulting deformations will not be identical along the ribbons of both α- and β-NCP (Fig. 3).

As can be deduced from the data of Table 3, sodium cations of α-$Na_2CuP_2O_7$ are located in two different sites corresponding to a coordination number (CN) of 8 for Na(1) and 6 for Na(2). The bond length Na–O ranges from 2.241 to 2.981 Å with a mean value of 2.559 Å for Na(1) and from 2.395 to 2.719 Å with a mean value of 2.500 Å for Na(2). Even though the coordination numbers are not identical in all compounds, the latter values are rather close to those found for other diphosphates containing sodium cations like $Na_2CoP_2O_7$, $Na_4P_2O_7$, etc. (3–5, 12, 39).

In the case of β-NCP, all sodium atoms are six-coordinated with Na–O bond lengths varying from 2.296 to 2.645 Å with a mean value of 2.424 Å. They are slightly longer than those found in $Na_2PdP_2O_7$ whose structure contains equivalent corrugated ribbons made of alternating $(P_2O_7)^{4-}$ groups and $[PdO_4]$ squares (17). Similar distances

TABLE 4
Main Interatomic Distances (Å) and Angles (°) for β-$Na_2CuP_2O_7$

$Cu-O^{i}(1) = 1.910(1)$ (2×)	$O^{i}(1)-Cu-O^{ii}(3) = 86.47(9)$
$Cu-O^{ii}(3) = 1.963(1)$ (2×)	$\langle Cu-O\rangle = 1.937$
$Na-O^{viii}(1) = 2.341(1)$	$Na-O^{vii}_{010}(2) = 2.296(2)$
$Na-O^{i}(2) = 2.327(2)$	$Na-O^{ii}_{010}(3) = 2.645(2)$
$Na-O^{ii}_{010}(2) = 2.543(2)$	$Na-O^{vii}(3) = 2.393(1)$
	$\langle Na-O\rangle = 2.424$
$P-O^{i}(1) = 1.523(2)$	$O^{i}(1)-P-O^{i}(2) = 112.84(19)$
$P-O^{i}(2) = 1.492(1)$	$O^{i}(1)-P-O^{i}(3) = 111.40(21)$
$P-O^{i}(3) = 1.535(2)$	$O^{i}(1)-P-O^{i}(4) = 105.75(13)$
$P-O^{i}(4) = 1.616(1)$	$O^{i}(2)-P-O^{i}(3) = 111.82(16)$
$\langle P-O\rangle = 1.542$	$O^{i}(2)-P-O^{i}(4) = 107.75(12)$
	$O^{i}(3)-P-O^{i}(4) = 106.84(15)$
	$\langle O-P-O\rangle = 109.40$
	$\langle P-O(4)-P\rangle \approx 120.2(1)$

Note. Symmetry code (see Table 2 for the values of x, y, z): (i) $x\ y\ z$; (ii) $x(\frac{1}{2}-y)(\frac{1}{2}+z)$; (iii) $\bar{x}\ \bar{y}\ \bar{z}$; (iv) $\bar{x}\ y(\frac{1}{2}-z)$; (v) $(\frac{1}{2}+x)(\frac{1}{2}+y)z$; (vi) $(\frac{1}{2}+x)(\frac{1}{2}-y)(\frac{1}{2}+z)$; (vii) $(\frac{1}{2}-x)(\frac{1}{2}-y)z$; (viii) $(\frac{1}{2}-x)(\frac{1}{2}+y)(\frac{1}{2}-z)$.
$O^{X}_{pqr}(n)$ represents the oxygens $O(n)$ concerned with the above symmetry code X and the translation vector $p\mathbf{a} + q\mathbf{b} + r\mathbf{c}$.

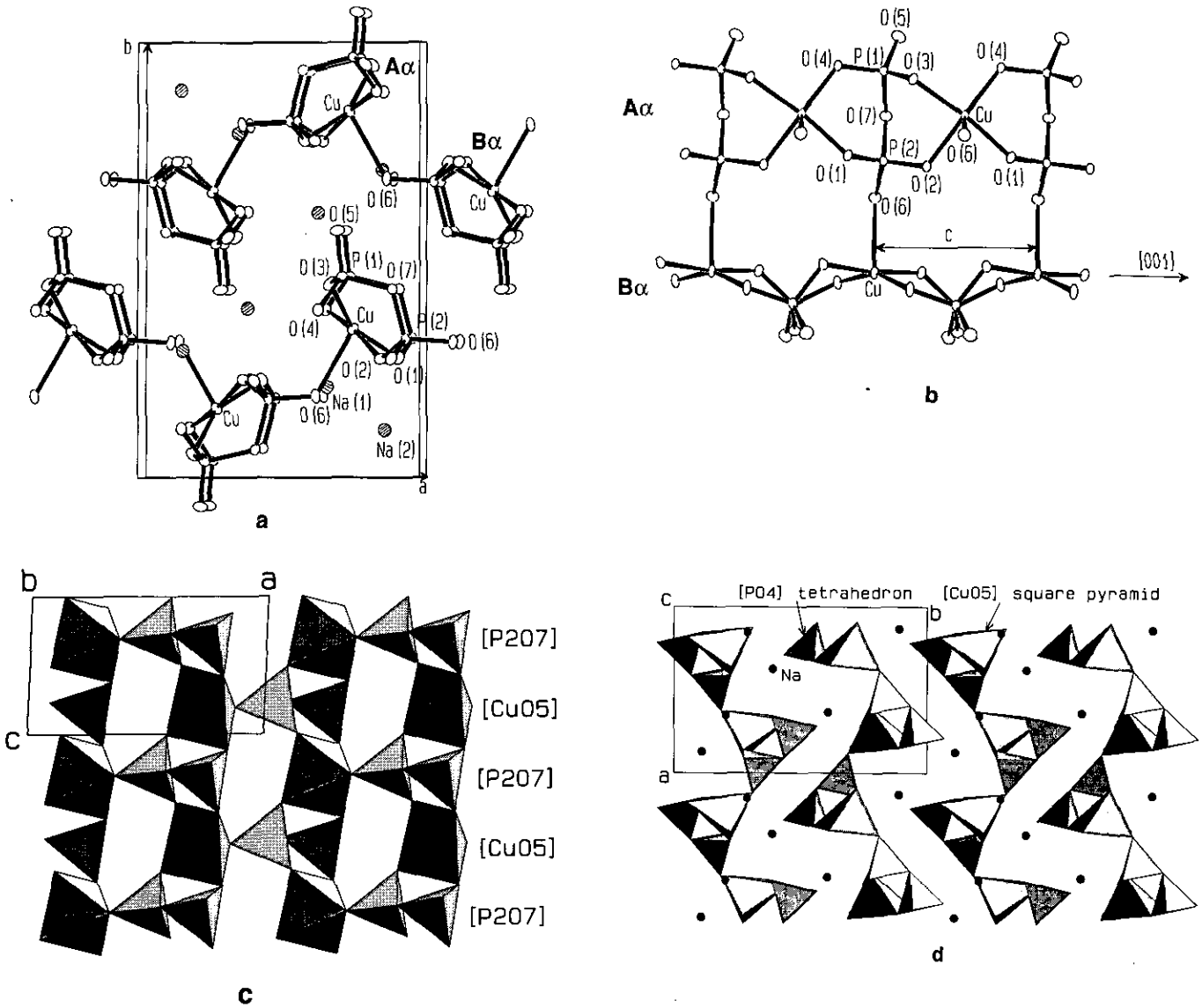

FIG. 1. Structure of α-$Na_2CuP_2O_7$: (a) projection of the unit cell along [001]; (b) projection of two adjacent ribbons A_α and B_α and their junctions through Cu–O(6) bonds; (c) arrangement of diphosphate groups and copper square pyramids within a corrugated layer; (d) stacking of the corrugated layers linked by sodium cations.

were observed in $Na_4P_2O_7$ and the high-temperature form of $NaFeP_2O_7$ (39, 40).

The analysis of Na–O distances in the vicinity of Na(1) and Na(2) shows that the main value ⟨Na(1)–O⟩ corresponding to a CN = 8 is larger than ⟨Na(2)–O⟩ corresponding to CN = 6. These results are compatible with the well-known variation of ionic radii versus coordination number, formerly reported by Shannon and Prewitt for oxydes and fluorides (41). Nevertheless, the mean value of Na–O, equal to 2.424 Å in the case of β-NCP, is much lower than ⟨Na(1)–O⟩ of α-NCP, even though both sodium atoms are located in octahedral sites. It is also noteworthy that sodium cations occupy highly distorted cavities in both polymorphs of $Na_2CuP_2O_7$ as evidenced from the data given in Tables 3 and 4.

V. THERMAL STABILITY AND PHASE TRANSITIONS

The prominent differences between the crystal structures of the two polymorphs α- and β-$Na_2CuP_2O_7$ reside in the shape of the ribbons $[CuP_2O_7]_n^{2n-}$ (flat in α and corrugated in β) and the way the sodium cations are arranged between these strips (Figs. 1–3). Furthermore, it also has to be noticed that the main structural difference between the α and β networks could be attributed to the fact that the first one is a corrugated layer structure and

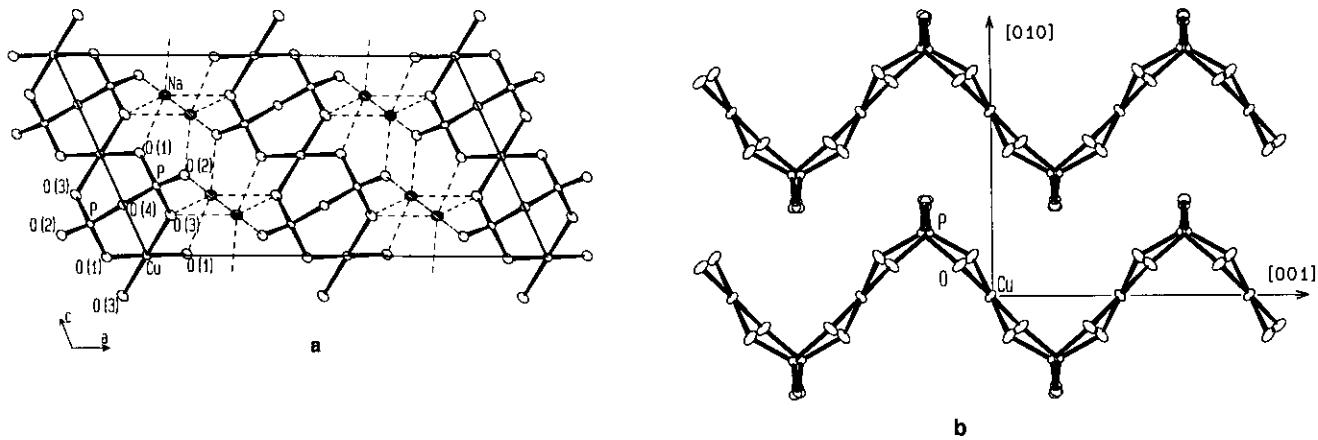

FIG. 2. View of β-$Na_2CuP_2O_7$ structure: (a) as projected on (010); (b) within the plane (100).

the second one is a ribbon layer. Due to the relatively short Cu–O(6) distance (2.388 Å), the ribbons of α-NCP appear as strongly anchored to each other through these bonds while equivalent bonds are almost inexistent in the β-phase because the corresponding distances are too long. However, due to Van der Waals weak bonds, the ribbons of the latter modification are stacked within layers (Fig. 2) cemented by sheets of sodium cations parallel to (100).

Thus it appears clearly from the preceding discussions that both transformations of α into β and vice versa should result in a total atomic reorganization within the whole lattice (Fig. 3): $(P_2O_7)^{4-}$ groups should change their orientation in order to be adapted to the type of ribbons (corrugated or not) implicated in the structure that emerges during the phase transition. Accordingly sodium cations must also diffuse either from or to the foregoing layers depending on the variety to be reached, α- or β-$Na_2CuP_2O_7$. Moreover, a thermal variation of X-ray diffraction patterns has shown that the low-temperature allomorph (α-NCP) can transform, on heating, to the high-temperature form β-$Na_2CuP_2O_7$. Figure 4 shows that the phase transition $\alpha \rightarrow \beta$ takes place at about 860 K. In contrast, all attempts to convert β into α have remained unsuccessful despite the long periods of anealing at various temperatures ranging

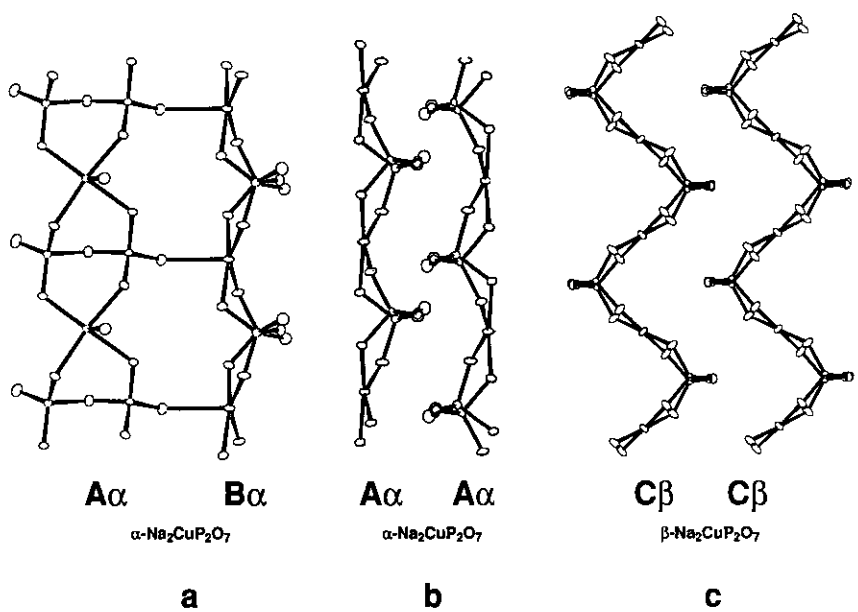

FIG. 3. Arrangement of various ribbons: (a) A_α and B_α related by the glide plane n in α-$Na_2CuP_2O_7$. The planes of A_α and B_α running along [001] are perpendicular; (b) of the same type (A_α or B_α) parallel and related by an inversion center; (c) C_β (corrugated) in β-$Na_2CuP_2O_7$.

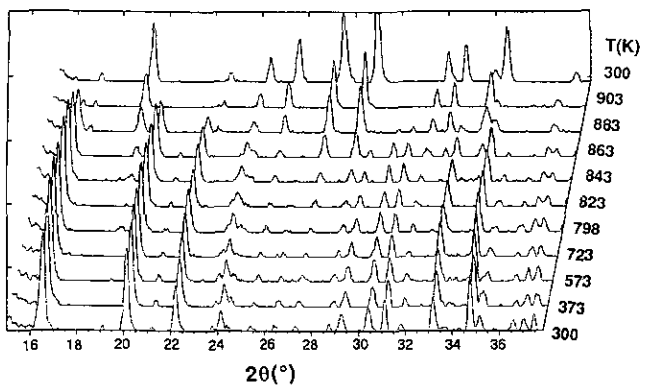

FIG. 4. Thermal variation of X-ray diffraction patterns recorded on a pulverulent sample of α-$Na_2CuP_2O_7$ from 300 to 903 K.

below 860 K. Furthermore, it was not possible to prepare pulverulent α-NCP by a standard solid-state synthesis technique neither from mixtures of $Na_4P_2O_7$ and $Cu_2P_2O_7$ nor from that of CuO, $(NH_4)_2HPO_4$, and Na_2CO_3, even though all heat treatments were achieved at temperatures lower than 860 K. The only way to synthesize this phase seems to be the one described in Section II(a). It then appears clearly that both α- and β-$Na_2CuP_2O_7$ are very stable at room temperature once they are prepared.

The irreversible character of the transformation $\alpha \rightarrow \beta$ has been tentatively explained as follows:

—Concerning $\alpha \rightarrow \beta$ transition: rising the temperature of α-$Na_2CuP_2O_7$ was considered as accompanied by increasing atomic vibrations and particularly sodium cations which then tend to diffuse within the lattice. At the transition temperature, the thermal agitation can probably be considered large enough to allow (a) the rupture of some bonds like Cu–O(6) and the elongation of the P–O–P bridges in order to favor their reorientation necessary for the corrugation of the ribbons $[CuP_2O_7]_n^{2n-}$; (b) the diffusion of Na^+ cations from their initial sites in α-phase in order to let free space for the folded ribbons to stack in layers parallel to (100). The latter are also parallel to the sheets where sodium atoms spread out after a total conversion of α- into β-$Na_2CuP_2O_7$.

—Concerning $\beta \rightarrow \alpha$ transition: provided this transition should take place, it has to be below or at 860 K as shown in Fig. 4. Nevertheless, some crystal chemical considerations can be advanced to justify why the transformation of $\beta \rightarrow \alpha$ appears to be very hard if not impossible to realize in spite of the many heat treatments carried out at various temperatures lower than 860 K. As a matter of fact, due to the reconstructive character of the $\alpha \rightarrow \beta$ transition formerly discussed, the inverse conversion $\beta \rightarrow \alpha$ would require important atomic reorganizations within the β-lattice. Obviously, large atomic displacements are needed in order to remove sodium cations from their sheets on the one hand and to flatten the corrugated ribbons and adjust their orientation according to the α-NCP lattice on the other hand. Furthermore, the bond length Na–O averages 2.427 Å in the β-phase while in the α-form, the mean values of Na(1)–O and Na(2)–O are equal to 2.559 Å and 2.500 Å, respectively. Since Na–O bonds are stronger in β- than in α-$Na_2CuP_2O_7$, it appears clearly that the transition from α to β will require more energy than the reverse transformation, to get sodium cations involved in such structural change. All other atomic displacements previously reported evidently require an important amount of energy furnished in the present case by the heat treatment. In the case of the $\alpha \rightarrow \beta$ transformation, rising the temperature is in favor of the stabilization of the β-phase. However, since the α-form is a low-temperature modification, achieving $\beta \rightarrow \alpha$ below 860 K will likely not provide all of the thermal energy necessary for the displacement of the appropriate atoms toward their final positions. This is probably the reason why we were not able to accomplish the $\beta \rightarrow \alpha$ transformation under the experimental conditions described above.

REFERENCES

1. A. Elayachi, Mémoire de C.E.A., Faculty of Science, Rabat, 1984.
2. F. Erragh, Mémoire de C.E.A., Faculty of Science, Rabat, 1985.
3. F. Erragh, Thèse de DES de3ème Cycle, Faculty of Science, Rabat, 1989.
4. F. Erragh, A. Boukhari, B. Elouadi, and E. M. Holt, *J. Crystallogr. Spectrosc. Res.* **23,** 321 (1991).
5. S. Aqdim, Thèse de DES de3ème Cycle, Faculty of Science, Rabat, 1990.
6. F. Erragh, A. Boukhari, F. Abraham, and B. Elouadi, to be published.
7. M. Ouchetto, Thèse de DES de 3ème Cycle, Faculty of Science, Rabat, 1983.
8. E. Arbib, Thèse de DES de 3ème Cycle, Faculty of Science, Rabat, 1988.
9. B. Elouadi, M. Ouchetto, E. Arbib, and N. Amraoui, *Phase Transitions* **13,** 219 (1988).
10. N. Amraoui, Thèse de DES de 3ème Cycle, Faculty of Science, Rabat, 1991.
11. J. Majling and F. Hanic, *J. Solid State Chem.* **7,** 370 (1973).
12. F. Hanic and Z. Zak, *J. Solid State Chem.* **10,** 12 (1974).
13. M. T. Averbuch-Pouchot, *Bull. Soc. Fr. Minéral. Cristallogr.* **95,** 513 (1972).
14. M. Gabelica-Robert, *C.R. Acad. Sci. Paris, Sér. II* **293,** 497 (1981).
15. A. Rulmont, P. Tarte, and J. M. Winand, *Eur. J. Solid State Inorg. Chem.* **28,** 1021 (1991).
16. Y. Laligant, *Eur. J. Solid State Inorg. Chem.* **29,** 239 (1992).
17. Y. Laligant, *Eur. J. Solid State Inorg. Chem.* **29,** 83 (1992).
18. J. Majling, S. Palco, F. Hanic, and T. Petrovic, *Chem. Zvesti.* **28,** 294 (1974).
19. I. D. Sokolova, I. S. Shaplyagin, G. A. Sharpataya, and I. B. Markina, *Russ. J. Inorg. Chem.* **28**(1), 18 (1983).
20. S. I. Berul and N. K. Voskresenskaya, *Inorg. Mater. (USSR)* **4**(12), 1855 (1968).
21. V. B. Lazarev, L. D. Sokolova, G. A. Sharpataya, I. S. Shaplygin, and I. B. Markina, *Thermochim. Acta* **86,** 243 (1985).
22. R. Klement, *Chem. Ber.* **93,** 2314 (1960).

23. J. Meulenaer and H. Tompa, *Acta Crystallogr.* **12,** 1014 (1965).
24. "International Tables for X-ray Crystallography" Vol. IV. Kynoch Press, Birmingham, UK, 1974.
25. D. T. Cromer and D. Liberman, *J. Chem. Phys.* **53,** 1891 (1970).
26. C. T. Pewitt, "SFL S-5, Report ORNL-TM 305", Oak Ridge National Laboratory, Oak Ridge, Tennessee, 1966.
27. R. J. Gillespie, "Molecular Geometry." Van Nostrand Reinolds, London, 1972.
28. D. W. J. Cruickshank, *J. Chem. Soc.* 5486 (1961).
29. M. Ouchetto, "Elaboration et études structurale, chimique et thermique des phases vitreuses des systèmes ternaires Li_2O–BO–P_2O_5 et ZnO–L_2O_3–P_2O_5 (B = Zn, Cd; L = La, Nd, Er, Yb, Bi)—Analyse de la liaison chimique et propriétés diélectriques," Thèse de Doctorat d'état ès science, Faculty of Science, Rabat, 1993.
30. A. G. Nord and P. Kierkegaard, *Chem. Scr.* **15,** 27 (1980).
31. D. Riou, Ph. Labbe, and M. Goreaud, *Eur. J. Solid State Inorg. Chem.* **25,** 215 (1988).
32. A. Moqine, A. Boukhari, and E. M. Holt, *Acta Crystallogr. Sect. C* **47,** 2294 (1991).
33. M. Ijjaali, G. Venturini, R. Gerardini, B. Malman, and C. Gleitzer, *Eur. J. Solid State Inorg. Chem.* **28,** 983 (1991).
34. H. Effenberger, *Acta Crystallogr. Sect. C* **46,** 691 (1990).
35. S. Gali and K. Byrappa, *Acta Crystallogr. Sect. C* **46,** 2011 (1990).
36. M. T. Averbuch-Pouchot and A. Durif, *Acta Crystallogr. Sect. C* **48,** 973 (1992).
37. I. D. Brown and C. Calvo, *J. Solid State Chem.* **1,** 173 (1970).
38. A. F. Wells, "Structural Inorganic Chemistry," 5th ed. Oxford Univ. Press, London, 1990.
39. K. Y. Leung and C. Calvo, *Can. J. Chem.* **50,** 2519 (1972).
40. M. Gabelica-Robert, M. Goreaud, Ph. Labbe et B. Raveau, *J. Solid State Chem.* **45,** 389 (1982).
41. R. D. Shannon and C. T. Prewitt, *Acta Crystallogr. Sect. B* **25,** 925 (1969).